crystals

MDPI

Article

Influence of Austenitisation Time and Temperature on Grain Size and Martensite Start of 51CrV4 Spring Steel

Anže Bajželj [1,2] and Jaka Burja [1,2,*]

[1] Institute of Metals and Technology, 1000 Ljubljana, Slovenia
[2] Department for Materials and Metallurgy, Faculty of Natural Sciences and Engineering, University of Ljubljana, 1000 Ljubljana, Slovenia
* Correspondence: jaka.burja@imt.si

Abstract: 51CrV4 spring steel is a martensitic steel grade that is heat treated by quenching and tempering. Therefore, austenitisation is an important step that influences steel properties. The main goal of austenitisation is to obtain a single-phase austenite structure that will transform into martensite. We studied the influence of austenitisation parameters on grain growth and martensite transformation temperatures. The samples were quenched from different austenitisation temperatures (800–1040 °C) and were held for 5, 10 and 30 min. The martensite start transformation temperatures (M_S) were determined from dilatometric curves, and the hardness was measured using the Vickers method. The microstructure of the samples and the size of the prior austenite grains were characterised using optical microscopy. The increase in the size of the prior austenite crystal grains increases the M_S temperature. However, this trend is visible up to 960 °C, where the results start to deviate. High temperatures, 960 °C and above, cause both grain growth and increased carbide dissolution along with chemical homogenization of the steel. The added influence of strong solute diffusion caused a big deviation in the results. The stability of carbides during austenitisation were evaluated with scanning electron microscopy (SEM) and thermodynamic calculations of equilibrium phases using the Thermo-Calc program. MC-type vanadium carbides are stable up to 956 °C under equilibrium conditions, but the SEM results show that they were present in the microstructure even after annealing at 1040 °C. This means that crystal growth is slowed down, which is positive, and that the austenite contains less carbon, so the hardness is lower.

Keywords: spring steel; martensite; grain growth; martensite start; dilatometry; austenitisation

Citation: Bajželj, A.; Burja, J. Influence of Austenitisation Time and Temperature on Grain Size and Martensite Start of 51CrV4 Spring Steel. *Crystals* **2022**, *12*, 1449. https://doi.org/10.3390/cryst12101449

Academic Editors: Mingyi Zheng, Tilen Balaško, Barbara Šetina Batič and Aleš Nagode

Received: 28 September 2022
Accepted: 11 October 2022
Published: 13 October 2022

1. Introduction

Spring steels are the most commonly used materials in springs, as they have high fatigue resistance and high tensile strength [1–6]. Fatigue can be described as a localised progressive crack growth that occurs under fluctuating stresses. The stresses that cause fatigue failure are well below the yield strength. Some alloys such as most steels and Ti alloys exhibit a fatigue or endurance limit where a certain stress can be applied indefinitely and will not cause failure, while others like Al and Cu alloys do not have an endurance limit. The combination of high strength and endurance limit is therefore desirable for spring applications [7,8]. Steels used for springs range from high-carbon low-alloyed, medium-carbon alloyed to stainless steels. They are always heat treated to achieve mechanical properties, and the most common treatment is quenching and tempering [9,10]. Although heat treatment is a broad topic and used in many alloys for different purposes, from age hardening to dissolution of deleterious phases, hardening steels by quenching and subsequent tempering is one of the most widely spread heat treatment protocols. Heat treatment is especially important for achieving reliable results after material processing, such as after hot forming or welding [7,8,11–14]. When quenching and tempering, it is important to carefully plan the austenitisation process. It is necessary to determine the

appropriate temperature and time of the austenitisation in order to achieve a homogeneous single-phase state (single-phase austenite region and uniform distribution of alloying elements), while it is necessary to ensure that the austenite crystal grains do not grow excessively, which would negatively affect the mechanical properties of steels [8,15,16]. Austenite transformation and crystal grain growth are diffusion-controlled processes that depend on temperature and time.

To predict the growth of crystal grains, a series of theoretical and semi-empirical models have been derived, which include thermodynamic parameters of steels and describe the migration of crystal boundaries during the austenitisation process as functions of temperature and time [17–22]. In low-carbon low-alloyed steels, the kinetics of crystal grain growth increases with temperature, and crystal grain migration decreases with the addition of alloying elements. The movement of crystal grains can be slowed down due to the segregation of alloying elements at the crystal boundaries (the solute drag effect), and due to undissolved precipitates (carbides, nitrides), so called pinning effect is cancelled at the moment when the particles dissolve in the matrix and the kinetics of grain growth is accelerated [15,19,21,23–28].

The selection of appropriate austenitisation parameters is crucial for the martensitic transformation. The homogeneity of the microstructure and the size of the crystal grains are parameters that influence the hardenability of steels. A good distribution of alloying elements and a homogeneous microstructure increase the activation energy for the martensitic transformation and increase the hardenability of the steel [29,30]. As stated by Lee et al. [18] and Lambers et al. [31], the hardenability of steel improves with crystal grain growth. The greater number of crystal boundaries, i.e., small crystal grain size, hinders the growth of martensite laths [32]. Additionally, Lambers et al. [31] stated that in steels with smaller crystal grains, the density of dislocations in austenite crystal grains increases faster, thus inhibiting the growth of martensite.

Spring steel 51CrV4 was used in the present work, the aim of the research was to analyse the influence of austenitisation temperature and time on the martensitic transformation in 51CrV4 steel. Additionally, an analysis of the presence of carbides and the growth of prior austenite crystal grains depending on the temperature and time of austenitisation was also carried out in the present research. Steel 51CrV4 was developed for use in quenched and tempered condition, where it exhibits good strength properties, and is tough and resistant to fatigue [4,33]. According to the manufacturers' instructions, steel is quenched in oil from a temperature of between 820 and 860 °C, followed by tempering between temperatures of 540 and 680 °C [34]. Later, it was found that steel in the bainite state can exhibit even better properties and, at the same time, is cheaper to manufacture [30,35].

2. Materials and Methods

The chemical composition of the 51CrV4 steel samples is given in Table 1 and was determined by optical emission spectroscopy using ARL 3460 (ThermoFisher Scientific, Waltham, MA, USA). The content of sulphur and carbon was determined with a LECO CS-600 combustion mass spectrometer (Leco Corporation, St. Joseph, MI, USA). Figure 1 shows the ferritic-pearlitic microstructure of the initial state sample etched with Nital (5 vol. %).

Table 1. Chemical composition of the studied 51CrV4 spring steel (wt. %).

C	Si	Mn	P	S	Cr	V	Mo	Cu	Fe
0.52	0.26	0.76	0.013	0.005	1.00	0.18	0.09	0.21	bal.

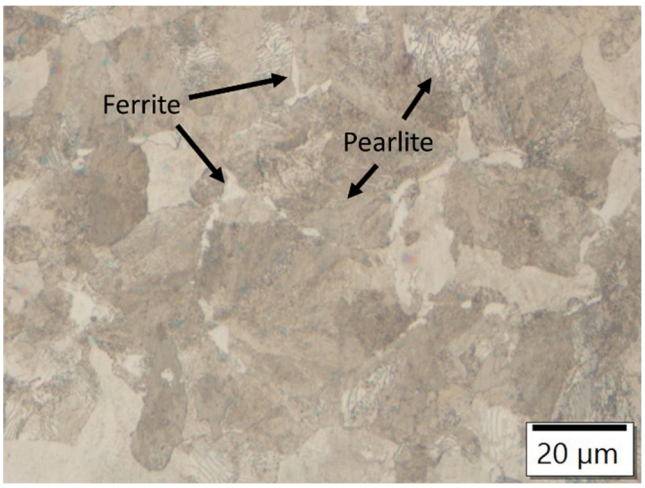

Figure 1. Ferritic–pearlitic microstructure of as received 51CrV4 steel sample, etched with 5 vol. % Nital.

Cylindrical samples with dimensions of Ø4 mm × 10 mm were made for dilatometry measurements. Measurements were performed with a TA DIL805A dilatometer (TA, New Castle, DE, USA) under vacuum and Ar atmosphere. Firstly, the transformation temperatures of the investigated steel were determined during heating and cooling in a vacuum up to 1000 °C. Heating and cooling rates of 0.05 and 10 K/s were used, respectively. In the second phase, an analysis of the influence of temperature and time of austenitisation on the size of the austenite crystal grains and the martensite start temperatures (M_S) took place. The samples were heated in a vacuum to 800, 860, 920, 960, 1000 and 1040 °C with a heating rate of 10 K/s, and were held at the temperature for 5, 10 and 30 min, respectively. This was followed by rapid cooling at a rate of 40 K/s in an Ar atmosphere. M_S temperatures were determined from the dilatometric cooling curves using the tangent method.

Dilatometry measurement samples were prepared for metallographic analysis, the cut samples were ground and polished, followed by etching with Nital (5 vol. %). The microstructure characterization was performed by Microphot FXA (Nikon, Minato City, Japan) with a 3CCD video camera Hitachi HV-C20A (Hitachi, Ltd., Tokyo, Japan). The prior austenite grain size was determined using the line intercept method. Scanning electron microscopy and EDS analysis was performed with a JEOL JSM-6500F electron microscope (Jeol, Tokyo, Japan). Vickers hardness (HV10) was measured on the metallographic samples using an Instron Tukon 2100B device (Wilson Instruments, Norwood, MA, USA).

Based on the chemical composition given in Table 1, the equilibrium phase composition as a function of temperature was calculated using the Thermo-Calc program. The TCFE8 Steels/Fe-alloys database was used for thermodynamic calculations.

3. Results and Discussion

3.1. Thermodynamic Analysis

Figure 2 shows the amount of thermodynamically stable phases in the temperature interval between 600 and 1100 °C in the investigated steel. The equilibrium transformation of austenite into ferrite begins at 759 °C, below 747 °C the ferrite and cementite phases (BCC_A1, Cementite) are formed; the transformation of austenite is completed at 724 °C. Below 956 °C, secondary vanadium carbides (FCC_A1#2) are formed, which are stable throughout the entire range presented in the figure. Figure 3 shows the chemical equilibrium composition and the amount of vanadium carbides between 600 and 956 °C. Besides vanadium and carbon, the particles also contain small amounts of Fe, Cr, Mo and Mn. At the end of the solidification process, as a result of the segregation of manganese and sulphur, MnS non-metallic inclusions are formed.

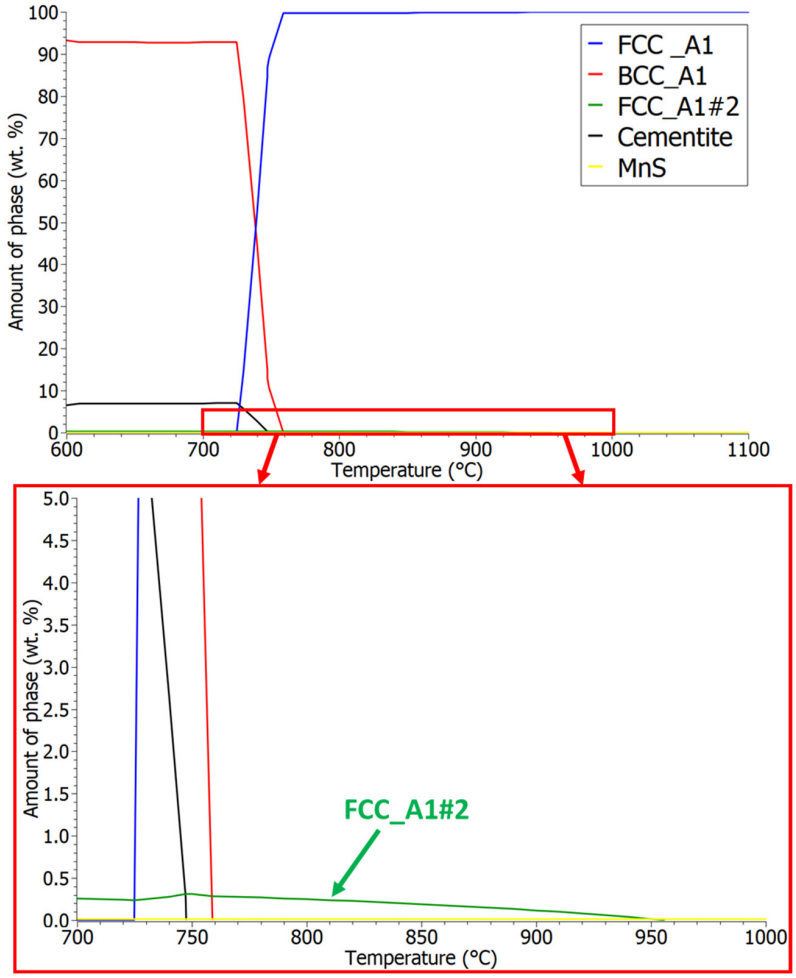

Figure 2. The equilibrium phase composition of 51CrV4 steel between 600 and 1100 °C.

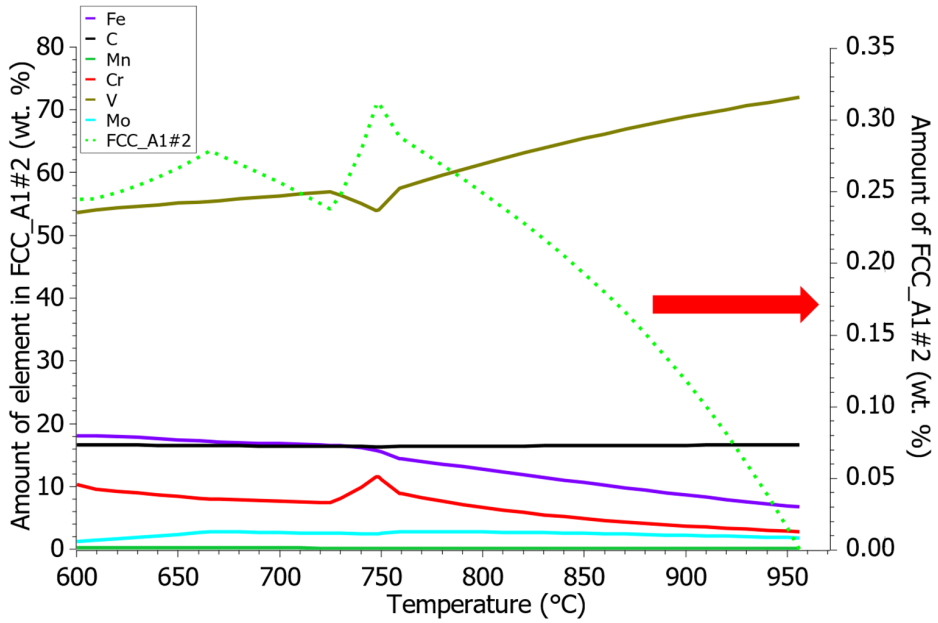

Figure 3. The equilibrium chemical composition of vanadium carbides (FCC_A1#2) and amount of precipitated FCC_A1#2 carbides (doted curve–right axis marked by red arrow) during cooling.

3.2. Transformation Temperatures

Figure 4 shows the dilatometric curves of the sample heated and cooled in vacuum at heating/cooling rate of 0.05 °C/s. The transformation temperatures A_{C1}, A_{C3}, A_{R1}, A_{R3} were 742 °C, 765 °C, 662 °C and 680 °C, respectively, which deviate from the equilibrium transformation temperatures A_{E1} (724 °C) and A_{E3} (759 °C) determined by the Thermo-Calc program. During heating, the transformation temperatures are expected to be higher than the equilibrium transformation temperatures, and during cooling, they are expected to be lower compared to the equilibrium transformation temperatures.

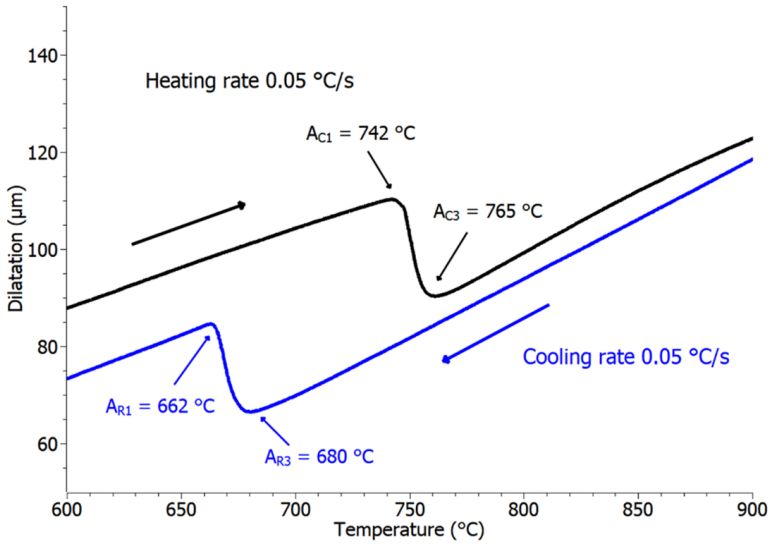

Figure 4. Determination of transformation temperatures at 0.05 °C/s heating and cooling rate.

A heating rate of 10 °C/s was used in the analysis of the influence of austenitisation temperature and time. Figure 5 shows the dilatometric curve of the heated sample at a given heating rate. By increasing the heating rate, the transformation temperatures A_{C1} and A_{C3} increased as well (775 °C and 805 °C) [36]. The transformation into austenite is diffusion-driven and therefore relatively slow, so the onset of the transformation is delayed at faster heating [37].

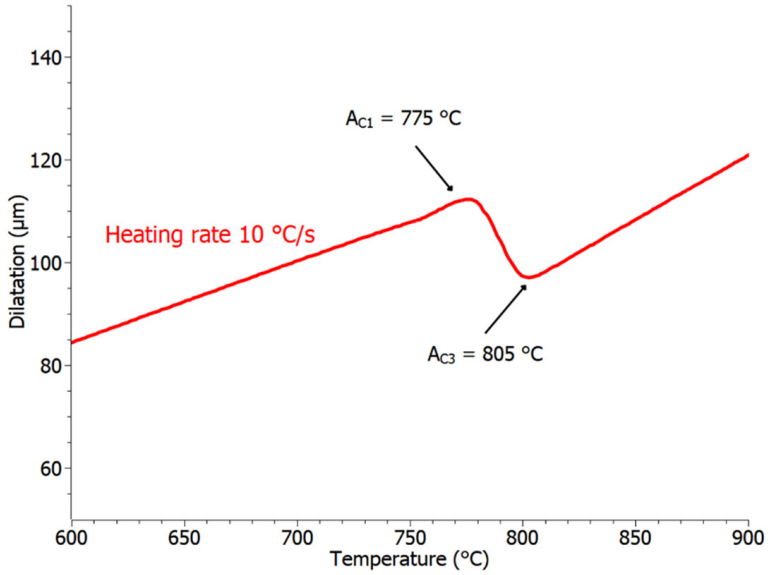

Figure 5. Determination of transformation temperatures at 10 °C/s heating rate.

3.3. Optical Microscopy

Figure 6a–d show the microstructures of the quenched samples from 800 and 1040 °C, after 5 and 30 min at the austenitisation temperature. The quenched samples consist of untempered lath martensite. As the time and temperature of austenitisation increases, the size of the austenite crystal grains increases and consequently, also the size of the martensite laths. The average sizes of the prior austenite crystal grains were estimated on the basis of microstructure images. The sizes of prior austenite grains are given in the diagram in Figure 7.

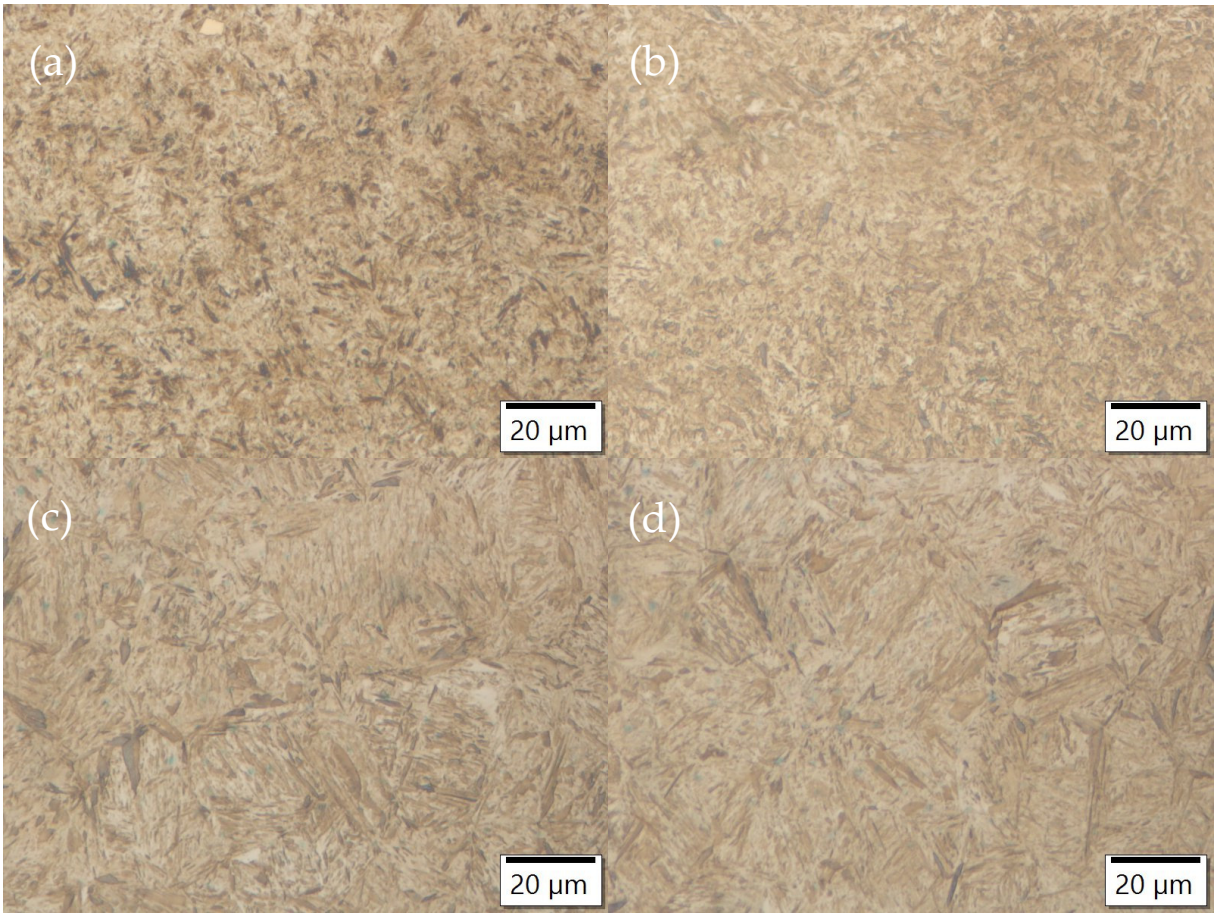

Figure 6. The microstructures of etched, quenched samples (**a**) 800 °C-5 min, (**b**) 800 °C-30 min, (**c**) 1040 °C-5 min and (**d**) 1040 °C-30 min.

Figure 8a,b show the microstructures of the quenched sample 1040 °C-30 min. Etching of the quenched samples revealed segregations in the microstructure resulting from the steelmaking process. The chemical segregations form during solidification, and are reduced by high temperature annealing and hot rolling, but they are typically still visible in the final product. Such chemical segregations are common for the continous casting and hot-rolling production route. Furthermore, special metallurgical processes such as electroslag remelting can almost completely eliminate segregations, but are, due to the high cost, used in the production of expensive materials such as tool steels. The austenitisation during dilatometry did not take place for enough time to eliminate the present segregations. In the samples, there were areas with more and less segregation bands, the distances between the segregation bands vary widely, indicating large chemical inhomogeneities in the material.

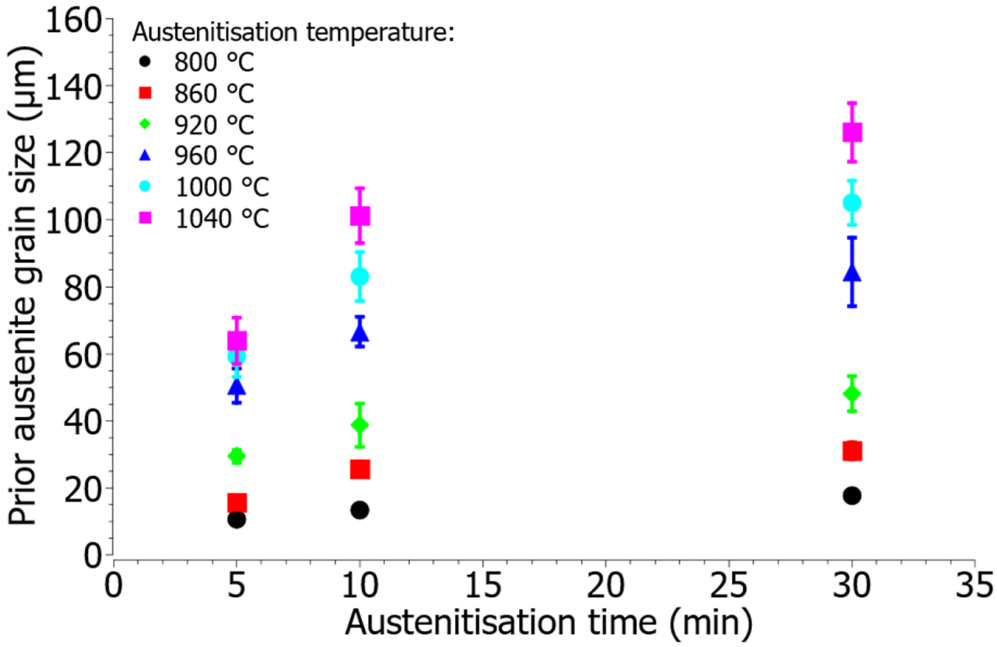

Figure 7. The size of the prior austenite grains.

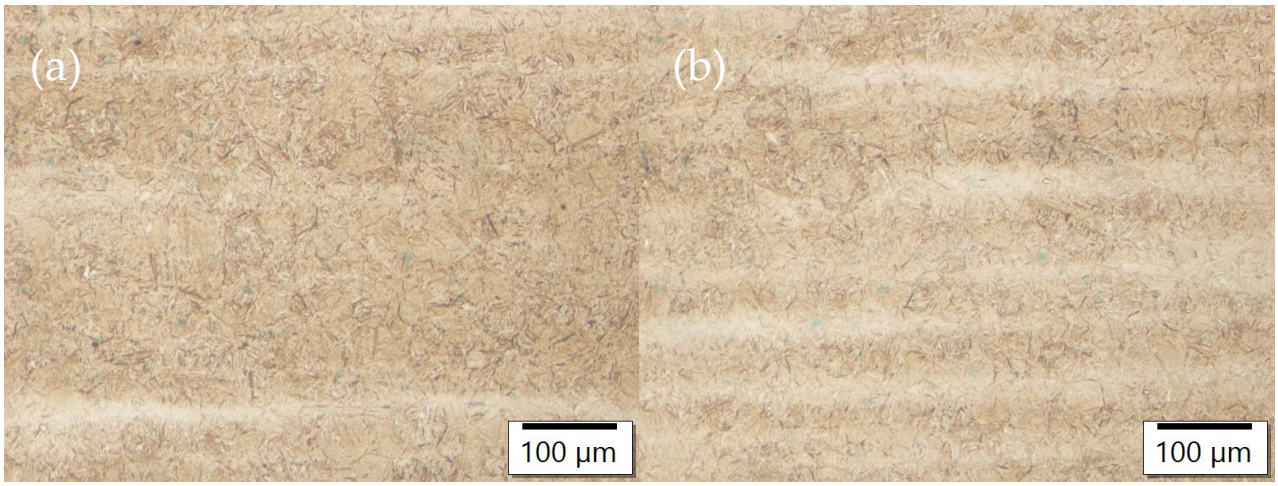

Figure 8. The microstructures of quenched sample 1040 °C-30 min, etched with Nital. (**a**) Area with less segregation bands, (**b**) area with more segregation bands.

3.4. Hardness

Figure 9 shows the results of the hardness measurement according to the Vickers method. The hardness of the quenched samples varies between 706 and 739 HV. For samples heated to 800 and 860 °C, a slight trend of increasing hardness with increasing austenitisation time was observed, which may be related to longer times for austenitic transformation, especially at 800 °C, and longer dissolution times of chromium and vanadium carbides and thus an increase in carbon concentration in the austenitic or martensitic matrix. According to Goulas et al. [30], vanadium carbides are stable up to 910 °C and chromium carbides slightly below. Samples heated above 920 °C were expected to dissolve the carbides completely in the matrix and, consequently, there was no tendency for the hardness to increase with increasing austenitisation time.

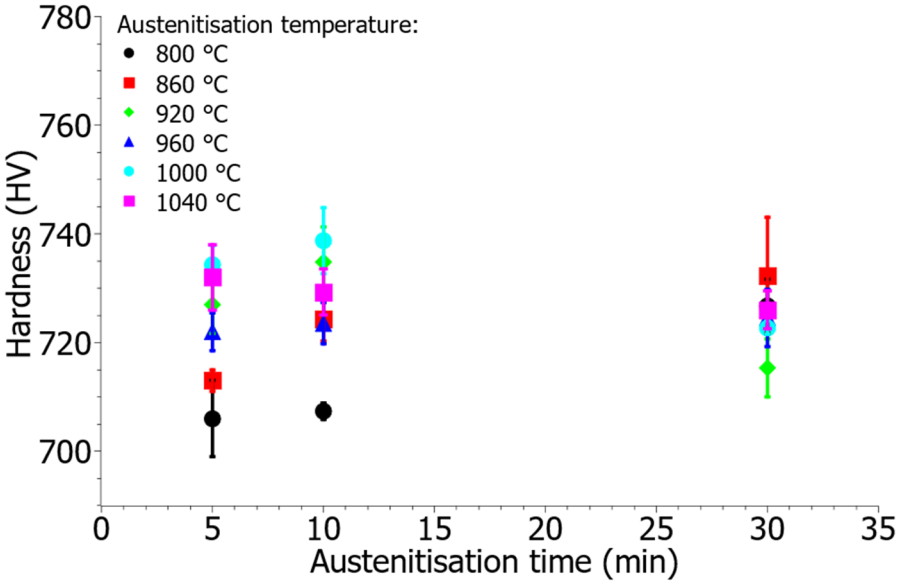

Figure 9. The hardness of the quenched samples.

3.5. Dilatometry and M_S Temperature

Figure 10a–f show dilatometric cooling curves of rapid cooling (40 °C/s) from different austenitisation temperatures (800, 860, 920, 960, 1000 and 1040 °C) and different austenitisation times (5, 10 and 30 min). A martensitic transformation occurred during rapid cooling; M_S temperatures were estimated on the basis of dilatometric curves. With the increase of the holding time at the temperature of 800 °C (Figure 10a), the temperature of M_S decreases. According to the dilatometry curve from Figure 5 the partial transformation to austenite occurred at the austenitisation temperature of 800 °C. With a longer austenitisation time, a greater proportion of the transformation takes place, and the distribution of alloying elements is accelerated, which affects the increase of the activation energy for the martensitic transformation [31]. However, at 800 °C, the grain size is not the dominant factor for the M_S, but rather the low dissolution of carbides (even cementite) and subsequently low carbon content. This will be presented in the SEM analysis section later on. At austenitisation temperatures 860 and 920 °C (Figure 10b,c) the M_S temperatures increase with increasing austenitisation time, mainly due to crystal grain growth. The degree of homogenisation and the concentration of alloying elements in the matrix increase with the increase of the austenitisation time and temperature, while at the same time there is a more intensive growth of crystal grains, which lowers the energy of shear displacements during the martensitic transformation [31]. At austenitisation temperatures above 960 °C (Figure 10d–f) and longer holding times (10 and 30 min) the M_S temperatures deviate obviously. At higher temperatures and longer times of austenitisation, the diffusion of alloying elements takes place more intensively, and due to the different degree of segregation and subsequent homogenisation of the material, there are greater deviations in M_S temperatures. These are shown in Figure 10d–f, where the two extremes are shown. It should be noted that austenitisation temperatures above 960 °C and shorter holding times (5 min), the M_S temperature are less scattered and increases mainly at the expense of the growth of prior austenite grains.

The scattering of the results for M_S in samples austenitised above 960 °C for more than 5 min is attributed to segregations, the associated uneven carbide dissolution and the partial homogenization process. At lower temperatures, grain size was the main difference, as grain growth was the dominant process. The grain size and M_S have a parabolic connection, as shown by Yang and Bhadeshia [38]; in our case, the connection seems linear, due to the small range, as shown in Figure 11. However, the connection is lost at higher temperatures and longer times, as mentioned before.

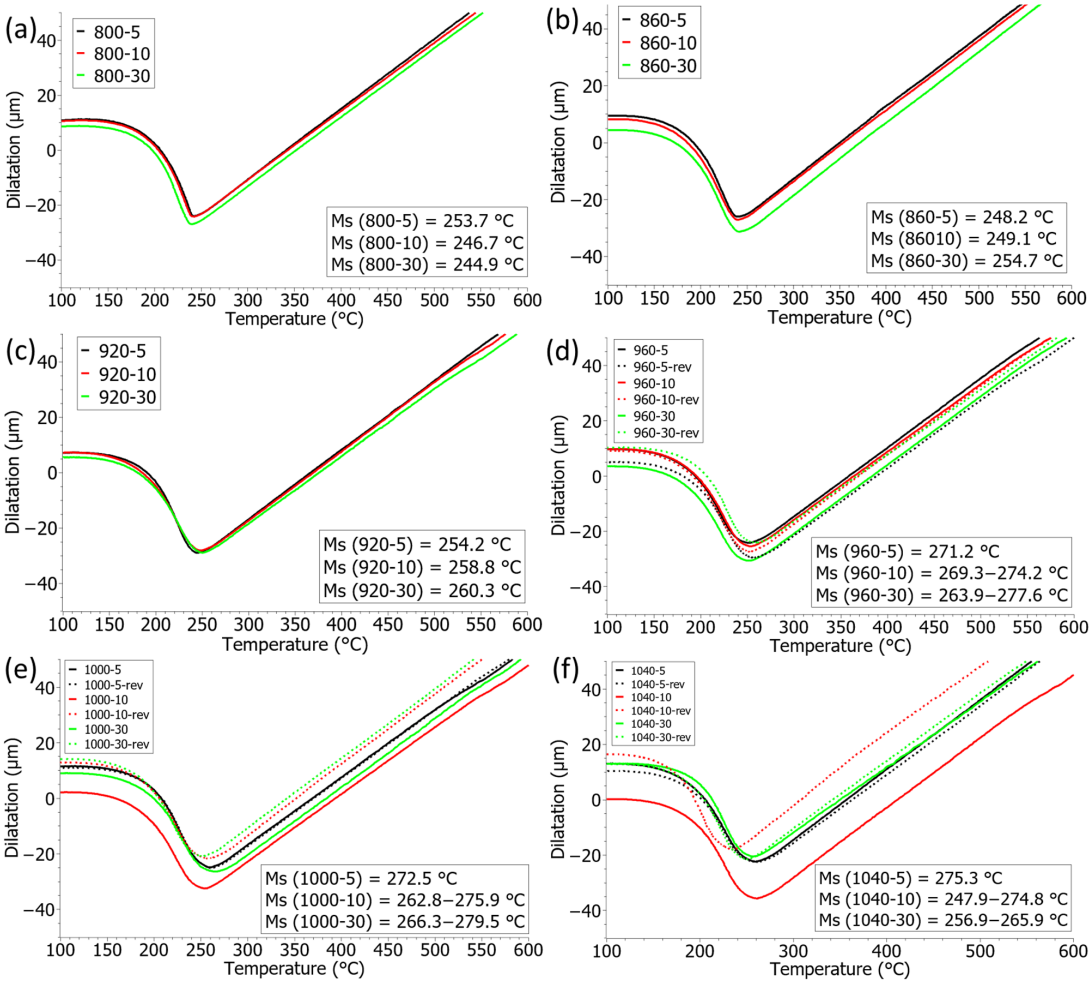

Figure 10. Dilatometric cooling curves from different austenitisation temperatures (**a**) 800 °C, (**b**) 860 °C, (**c**) 920 °C, (**d**) 960 °C, (**e**) 1000 °C, (**f**) 1040 °C.

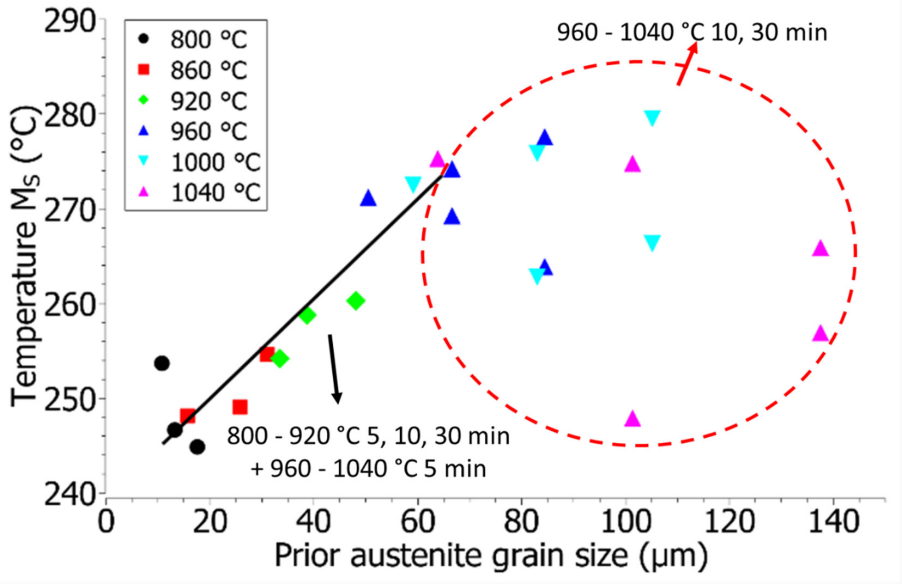

Figure 11. M_S and prior austenite gran size, the connection is clear at lower temperatures, and short term high temperature austenitisation, but the scattering becomes a problem at high temperatures and longer rimes.

3.6. Scanning Electron Microscopy

Figure 12a,b show SEM microscopy images of the quenched sample 800 °C-5 min. The spheroidised carbide particles indicate the remains of cementite lamellae, which is the result of a partial transformation of pearlite microstructure at a temperature of 800 °C. This explains the unusual drop in M_S temperature, supporting the explanation, given before, where the grain size is not the leading factor, but the austenite chemical composition. Figure 12c shows the microstructure of the sample 800 °C-30 min; the spheroidised carbide particles were not present in the sample; round carbides were distributed on the martensitic laths and near the prior austenite grain boundaries. Due to the small dimensions of the carbides, it is difficult to assess their exact chemical composition; based on thermodynamic calculations and EDS analysis, we can confirm that the carbide particles in 800 °C-5 min and 800 °C-30 min samples contain an elevated concentration of Cr, V, and Mo, which indicate the remains of cementite and MC-type carbides. As the temperature of austenitisation increases, the stability of carbides decreases, which coincides with the results of thermodynamic calculations and claims in the literature [29–31]. At austenitisation temperatures above 860 °C only undissolved secondary carbides rich in vanadium and chromium are present in the samples, they are mainly located at the boundaries of the prior austenite grains. The concentration and size of undissolved carbides decrease with the austenitisation temperature. At the austenitisation temperature of 1040 °C (Figure 12d–f), vanadium carbides are still in the microstructure, which is consequence of the local inhomogeneities in the microstructure.

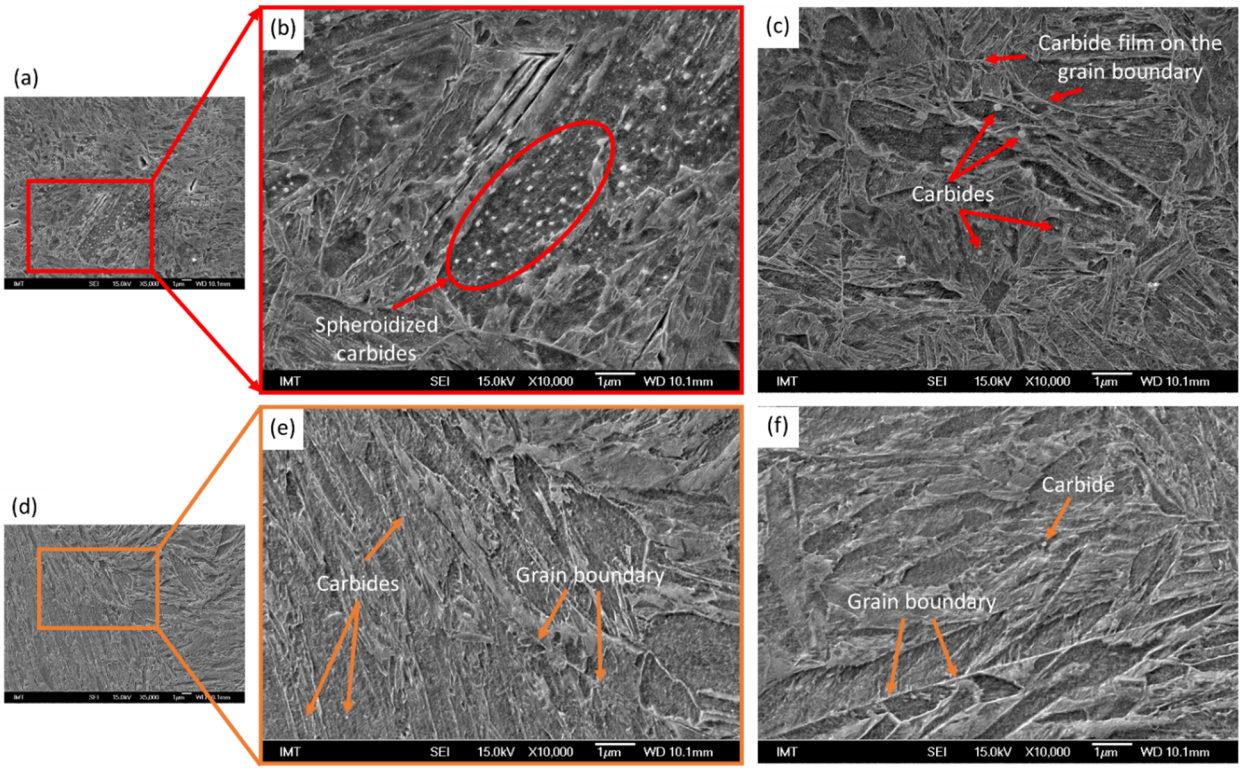

Figure 12. SEM images of quenched samples after 5 min at different austenitisation temperatures. (**a**) 800 °C-5 min lower magnification, (**b**) 800 °C-5 min, (**c**) 800 °C-30 min, (**d**) 1040 °C-5 min at lower magnification, (**e**) 1040 °C-5 min, (**f**) 1040 °C-30 min.

Figure 13a–c show a segregation band in the 1040 °C-30 min sample; despite the high austenitisation temperature and the longest holding time, segregations are still present in the microstructure. In the segregation zone, the concentration of alloying elements is increased and, as a result, the thermodynamic equilibrium in the segregation band is changed. In addition to oxide and sulphide non-metallic inclusions (NMI), there is also a large concentration of carbides in the segregation bands. The undissolved carbides partially

impair crystal growth, which is positive. However, the austenite consequently contains less carbon, which means lower hardness and slightly higher M_S.

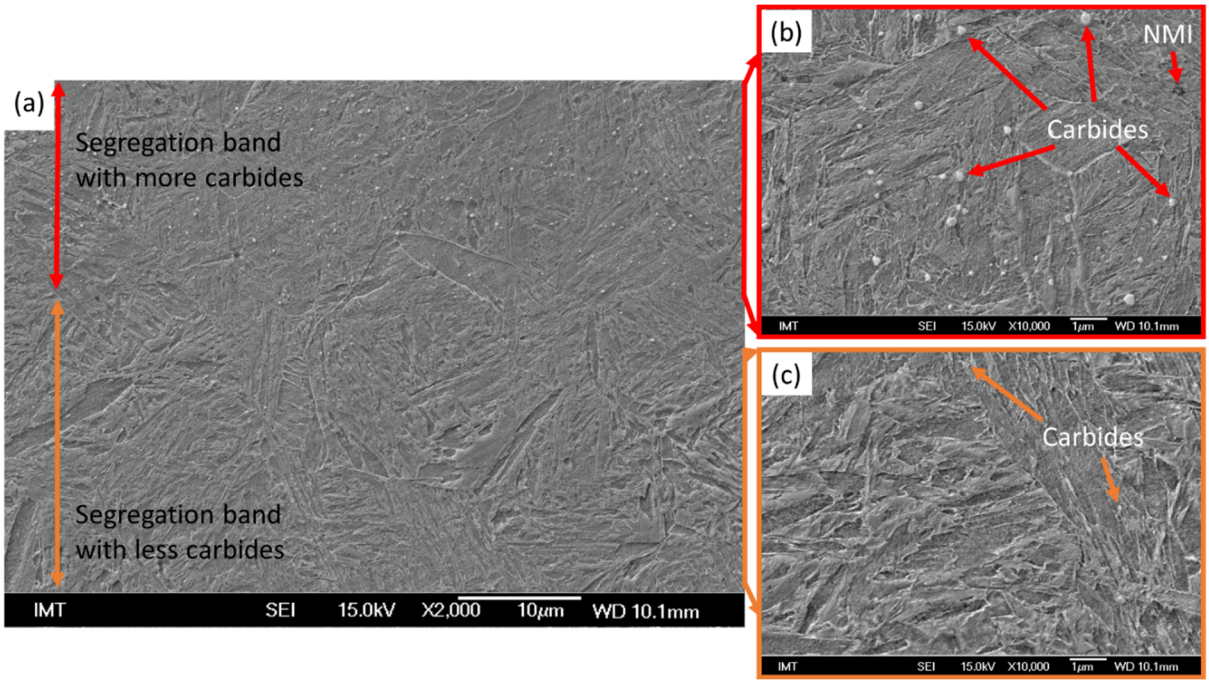

Figure 13. (**a**) SEM images of quenched 1040 °C-30 min sample at lower magnification, (**b**) segregation band, (**c**) area with less segregations. Notes: NMI—non-metallic inclusions.

4. Conclusions

The influence of austenitisation temperature and times on crystal grains growth, carbide dissolution and martensitic transformation of 51CrV4 spring steel were analysed. Austenitisation was carried out at temperatures between 800 and 1040 °C; the samples were held at the austenitisation temperature for 5, 10 and 30 min, followed by rapid cooling to room temperature. The following conclusions can be summarised:

- Prior austenite grains grow with increasing austenitisation temperature and times, with increasing temperature grain growth is more intense.
- The inhomogeneity of the microstructure can be observed in the quenched samples, which is the result of segregations during solidification. Due to the production route of the material, segregation bands with different distribution are present in the samples.
- At an austenitisation temperature of 800 °C, a partial transformation into austenite takes place; with a longer holding time at the temperature, a larger proportion of the transformation takes place, which affects the lowering of the martensite start temperature (M_S).
- In the case of complete austenitic transformation, the M_S temperature increases with the growth of crystal grains, and above 960 °C the M_S temperature is also affected by the distribution of alloying elements. Due to the more intensive diffusion of alloying elements and the different degree of distribution of segregations, there are greater deviations in the M_S temperature.
- Thermodynamic calculations using the Thermo-Calc program showed that the vanadium carbides in the investigated steel are stable up to 956 °C; using SEM, the vanadium carbides were analysed even at austenitisation temperatures of 1040 °C. The reason for the presence of carbides at such a high austenitisation temperature is local inhomogeneities and the limited time of carbide dissolution.

- There is an increased concentration of alloying elements in the segregation bands; the non-metallic inclusions and a higher concentration of carbides were characterised in the segregated areas.

Author Contributions: Conceptualization, A.B. and J.B.; methodology, J.B.; validation, A.B. and J.B.; formal analysis, J.B.; investigation, A.B.; writing—original draft preparation, A.B.; writing—review and editing, J.B.; visualization, A.B.; supervision, J.B.; All authors have read and agreed to the published version of the manuscript.

Funding: This research was funded by ARRS, grant number P2-0050.

Informed Consent Statement: Not applicable.

Data Availability Statement: Not applicable.

Conflicts of Interest: The authors declare no conflict of interest.

References

1. Chen, C.; Jiang, Z.; Li, Y.; Sun, M.; Wang, Q.; Chen, K.; Li, H. State of the Art in the Control of Inclusions in Spring Steel for Automobile—A Review. *ISIJ Int.* **2020**, *60*, 617–627. [CrossRef]
2. Totten, G.E. (Ed.) *Steel Heat Treatment Handbook: Metallurgy and Technologies*; Taylor & Francis: Portland, OR, USA, 2006.
3. Ishii, T.; Takahashi, K. Prediction of Fatigue Limit of Spring Steel Considering Surface Defect Size and Stress Ratio. *Metals* **2021**, *11*, 483. [CrossRef]
4. Zhang, L.; Gong, D.; Li, Y.; Wang, X.; Ren, X.; Wang, E. Effect of Quenching Conditions on the Microstructure and Mechanical Properties of 51CrV4 Spring Steel. *Metals* **2018**, *8*, 1056. [CrossRef]
5. Xia, B.; Wang, B.; Zhang, P.; Ren, C.; Duan, Q.; Li, X.; Zhang, Z. Improving the High-Cycle Fatigue Life of a High-Strength Spring Steel for Automobiles by Suitable Shot Peening and Heat Treatment. *Int. J. Fatigue* **2022**, *161*, 106891. [CrossRef]
6. James, M.N.; Hattingh, D.G.; Matthews, L. Embrittlement Failure of 51CrV4 Leaf Springs. *Eng. Fail. Anal.* **2022**, *139*, 106517. [CrossRef]
7. Campbell, F.C. *Elements of Metallurgy and Engineering Alloys*; ASM International: Materials Park, OH, USA, 2008.
8. Verhoeven, J.D. *Steel Metallurgy for the Non-Metallurgist*; ASM International: Materials Park, OH, USA, 2007.
9. Liu, F.; Chen, K.; Kang, C.; Jiang, Z.; Ding, S. Effects of V–Nb Microalloying on the Microstructure and Properties of Spring Steel under Different Quenching-Tempering Times. *J. Mater. Res. Technol.* **2022**, *19*, 779–793. [CrossRef]
10. Dai, Q.; Li, K.; Men, K.; Fang, Z.; Chen, W.; Yang, T.; Feng, C.; Wu, J.-M.; Misra, R.D.K. Effect of Vanadium on the Microstructure and Mechanical Properties of 2100mpa Ultrahigh Strength and High Plasticity Spring Steel Processed by a Novel Online Rapid-Induction Heat Treatment. *Met. Mater. Int.* **2022**, *28*, 4043687. [CrossRef]
11. Dewangan, S. Effect of Heat Treatment into Tensile Strength, Hardness and Microstructural Attributes of TIG Welded Ti-6Al-4V Titanium Alloy. *Aust. J. Mech. Eng.* **2022**, 1–10. [CrossRef]
12. Burja, J.; Šuler, B.; Češnjaj, M.; Nagode, A. Effect of Intercritical Annealing on the Microstructure and Mechanical Properties of 0.1C-13Cr-3Ni Martensitic Stainless Steel. *Metals* **2021**, *11*, 392. [CrossRef]
13. Celin, R.; Kafexhiu, F.; Klančnik, G.; Burja, J. Properties of the Simulated Coarse-Grained Microstructure of Quenched and Tempered High-Strength Steel. *Mater. Technol.* **2021**, *55*, 115–120. [CrossRef]
14. Dewangan, S.; Chattopadhyaya, S. Analysing Effect of Quenching and Tempering into Mechanical Properties and Microstructure of 304-SS Welded Plates. *Acta Metall. Slovaca* **2022**, *28*, 140–146. [CrossRef]
15. Speer, J.G.; Gaster, R.J. Austenitizing in steels. In *Steel Heat Treating Fundamentals and Processes*; Dossett, J., Totten, G.E., Eds.; ASM International: Materials Park, OH, USA, 2013; Volume 4A, pp. 309–316.
16. Savran, V. Austenite Formation in C-Mn Steel. Ph.D. Thesis, Delft University of Technology, Delft, The Nederlanden, 2009.
17. Pous-Romero, H.; Lonardelli, I.; Cogswell, D.; Bhadeshia, H.K.D.H. Austenite Grain Growth in a Nuclear Pressure Vessel Steel. *Mater. Sci. Eng. A* **2013**, *567*, 72–79. [CrossRef]
18. Lee, S.J.; Lee, Y.K. Effect of Austenite Grain Size on Martensitic Transformation of a Low Alloy Steel. *Mater. Sci. Forum* **2005**, *475–479*, 3169–3172. [CrossRef]
19. Lee, S.J.; Lee, Y.K. Prediction of Austenite Grain Growth during Austenitization of Low Alloy Steels. *Mater. Des.* **2008**, *29*, 1840–1844. [CrossRef]
20. Jafarian, H.R.; Sabzi, M.; Mousavi Anijdan, S.H.; Eivani, A.R.; Park, N. The Influence of Austenitization Temperature on Microstructural Developments, Mechanical Properties, Fracture Mode and Wear Mechanism of Hadfield High Manganese Steel. *J. Mater. Res. Technol.* **2021**, *10*, 819–831. [CrossRef]
21. Dong, D.; Chen, F.; Cui, Z. Modeling of Austenite Grain Growth During Austenitization in a Low Alloy Steel. *J. Mater. Eng. Perform.* **2016**, *25*, 152–164. [CrossRef]
22. Chamanfar, A.; Chentouf, S.M.; Jahazi, M.; Lapierre-Boire, L.P. Austenite Grain Growth and Hot Deformation Behavior in a Medium Carbon Low Alloy Steel. *J. Mater. Res. Technol.* **2020**, *9*, 12102–12114. [CrossRef]

23. Foder, J.; Burja, J.; Klančnik, G. Grain Size Evolution and Mechanical Properties of Nb, V–Nb, and Ti–Nb Boron Type S1100QL Steels. *Metals* **2021**, *11*, 492. [CrossRef]
24. Maropoulos, S.; Karagiannis, S.; Ridley, N. The Effect of Austenitising Temperature on Prior Austenite Grain Size in a Low-Alloy Steel. *Mater. Sci. Eng. A* **2008**, *483–484*, 735–739. [CrossRef]
25. Hong, S.C.; Lim, S.H.; Hong, H.S.; Lee, K.J.; Shin, D.H.; Lee, K.S. Effects of Nb on Strain Induced Ferrite Transformation in C-Mn Steel. *Mater. Sci. Eng. A* **2003**, *355*, 241–248. [CrossRef]
26. Adamczyk, J.; Kalinowska-Ozgowicz, E.; Ozgowicz, W.; Wusatowski, R. Interaction of Carbonitrides V(C,N) Undissolved in Austenite on the Structure and Mechanical Properties of Microalloyed V-N Steels. *J. Mater. Process. Technol.* **1995**, *53*, 23–32. [CrossRef]
27. Matsuo, S.; Ando, T.; Grant, N.J. Grain Refinement and Stabilization in Spray-Formed AISI 1020 Steel. *Mater. Sci. Eng. A* **2000**, *288*, 34–41. [CrossRef]
28. Devra, V.K.; Maity, J. Solute Drag Effect on Austenite Grain Growth in Hypoeutectoid Steel. *Philos. Mag. Lett.* **2020**, *100*, 245–259. [CrossRef]
29. Lambers, H.G.; Tschumak, S.; Maier, H.J.; Canadinc, D. Role of Austenitization and Pre-Deformation on the Kinetics of the Isothermal Bainitic Transformation. *Metall. Mater. Trans. A Phys.* **2009**, *40*, 1355–1366. [CrossRef]
30. Goulas, C.; Mecozzi, M.G.; Sietsma, J. Bainite Formation in Medium-Carbon Low-Silicon Spring Steels Accounting for Chemical Segregation. *Metall. Mater. Trans. A* **2016**, *47*, 3077–3087. [CrossRef]
31. Lambers, H.; Tschumak, S.; Maier, H.J.; Canadinc, D. On the Bainitic and Martensitic Phase Transformation Behavior and the Mechanical Properties of Low Alloy 51CrV4 Steel. *Int. J. Struct. Chang. Solids* **2011**, *3*, 15–27.
32. Klančnik, G.; Krajnc, L.; Nagode, A.; Burja, J. Isothermal Quenching of As-Cast Medium Carbon, High-Silicon AR Steel. *Materials* **2022**, *15*, 5595. [CrossRef]
33. Zhi, C.; Yuan, G.; Xian-Guo, Y.; Hong, G.; Yao, H.; Hai-Dong, Z.; Min-Na, Z. Enhanced Axial Tension-Tension Fatigue Resistance of a 51CrV4 Spring Steel by Cryogenic Treatment. *Rev. Chim.* **2021**, *72*, 138–151. [CrossRef]
34. Sij Group. SIQUAL 8159 Steel. Available online: https://steelselector.sij.si/steels/VCV150.html (accessed on 26 September 2022).
35. Kawulok, R.; Schindler, I.; Kawulok, P.; Rusz, S.; Opěla, P.; Mališ, M.; Vašek, Z.; Subíková, M.; Váňová, P. Effect of Plastic Deformation on CCT Diagram of Spring Steel 51CrV4. In Proceedings of the METAL 2015—24th International Conference on Metallurgy and Materials, Brno, Czech Republic, 3–5 June 2015; pp. 345–350.
36. Gaggiotti, M.; Albini, L.; di Nunzio, P.E.; di Schino, A.; Stornelli, G.; Tiracorrendo, G. Ultrafast Heating Heat Treatment Effect on the Microstructure and Properties of Steels. *Metals* **2022**, *12*, 1313. [CrossRef]
37. Moravec, J.; Nováková, I.; Vondráček, J. Influence of Heating Rate on the Transformation Temperature Change in Selected Steel Types. *Manuf. Technol.* **2020**, *20*, 217–222. [CrossRef]
38. Yang, H.S.; Bhadeshia, H.K.D.H. Austenite Grain Size and the Martensite-Start Temperature. *Scr. Mater.* **2009**, *60*, 493–495. [CrossRef]